An internal electric field and interfacial S-C bonds jointly accelerate S-scheme charge transfer achieving efficient sunlight-driven photocatalysis

Linlin Sun[a], Xiaoshuo Liu[b], Xiaohan Jiang[a], Yibing Feng[a], Xunlei Ding[c], Nan Jiang[d], Jigang Wang[a,e,*]

[a]*Jiangsu Key Laboratory of Advanced Metallic Materials, School of Materials Science and Engineering, Southeast University, Nanjing, 211189, PR China*

[b]*School of Energy and Power Engineering, North China Electric Power University, Baoding, 071003, PR China*

[c]*Institute of Clusters and Low Dimensional Nanomaterials, School of Mathematics and Physics, North China Electric Power University, Beijing 102206, PR China*

[d]*Collaborative Innovation Center for Cardiovascular Disease, Translational Medicine of Jiangsu, School of Pharmacy, Nanjing Medical University, Nanjing, 211166, PR China*

[e]*Xizang Engineering Laboratory for Water Pollution Control and Ecological Remediation, Xizang Minzu University, Xianyang, 712082, PR China*

* Corresponding author Tel: +86-25-52090235;
E-mail: wangjigang@seu.edu.cn.

1. Synthesis of flower-like ZIS and Sv-ZIS

The flower-like ZIS was synthesized by a simple one-step hydrothermal method. Specifically, CTAB (0.8 mM) was dispersed in deionized water (50 mL) and $ZnSO_4 \cdot 7H_2O$ (1 mM), $InCl_3 \cdot 4H_2O$ (2 mM) and TAA (8 mM) were added in an orderly manner with stirring at room temperature for 40 min to obtain a clear solution. Subsequently, the mixed solution was poured into stainless steel autoclave maintained at 160 °C for 16 h in the oven. The reaction product was centrifuged, washed with water and ethanol, dried at 60 °C and fully ground to obtain a yellow powder named ZIS. The availability of (Sv-ZIS) was processed by $N_2H_4 \cdot H_2O$. Typically, ZIS (100 mg) was evenly dispersed in 50 mL of deionized water, and then $N_2H_4 \cdot H_2O$ (5 mL) was added. The reactants were transferred to the stainless steel autoclave, which reacted at 200 °C for 5 h. Finally, the precipitate was centrifuged, washed and dried to obtain Sv-ZIS.

2. Device characterizations

The crystal structure and phase composition of the as-prepared materials were detected by an X-ray diffractometer (XRD, D8-Discover, Germany) equipped with the Cu- Kα radiation source. The scanning range of 2 theta was 10~80° and the scanning speed was 5°/min. Electron paramagnetic resonance (EPR) spectra and electron spin resonance (ESR) spectra were detected on the Bruker A300-10/12 electron paramagnetic resonance spectrometer. Fourier-transform infrared spectroscopy (FT-IR, Nicolet iS10) was employed to study the functional group structure of samples. The morphology and microstructure of the photocatalysts were analyzed by scanning electronic microscopy (SEM, Navo Nano SEM450) and transmission electron microscopy (TEM, Talos F200X), respectively. High-resolution transmission electron microscopy (HRTEM) images, selected area electron diffraction (SAED) patterns, mapping images and energy dispersive spectroscopy (EDS) images corresponding to Sv-ZIS/CN were

acquired from TEM instruments. The elemental valence and chemical bond structure were measured by X-ray photoelectron spectroscopy (XPS) with the model of ESCALAB 250xi (America) electron spectrometer. The optical properties were estimated by a Cary 5000 UV–vis–NIR spectrophotometer (Varian) equipped with an integrating sphere (diameter=110 mm). Photoluminescence (PL) spectra were measured with an FSL1000 fluorescence spectrophotometer (Edinburgh Instruments Ltd). N_2 adsorption–desorption isotherms were examined using the Brunauer−Emmett−Teller method on a Micromeritics ASAP 2020 HD88 instrument. The UV–vis spectrophotometer (Agilent Cary 8454) was used to measure the absorbance of tetracycline and H_2O_2 production.

3. Photo-electrochemical tests

The photochemical properties of the photocatalysts were measured on an electrochemical workstation (CHI 660E, Shanghai, China) using a standard three-electrode system. Platinum plate, saturated Ag/AgCl, as-prepared photocatalyst were applied to the counter electrode, reference electrode and working electrode, respectively. The working electrode was prepared by the following steps. In general, 5 mg powder samples were ultrasonically dispersed in 1 mL alcohol for 30 min, followed by 40 μL Nafion solution for another 30 min. Afterward, 20 μL of the above suspended droplets were placed on indium tin oxide (ITO) glass with an area of 1 cm^2 and then dried overnight at room temperature. Sodium sulfate (Na_2SO_4, 0.5 M) is selected as an electrolyte in a quartz vessel. The transient photocurrent response (TPR) was measured using a Xenon lamp (with 420 nm filter) as the light source.

4. Density functional theory (DFT) calculations

DFT was performed using the Vienna ab initio simulation package (VASP) [1], in which

projector augmented wave potentials are accepted to describe the valence electrons, and the Perdew-Burke-Ernzerhof functional is utilized to describe exchange-correlation interactions of electrons [2-3]. The Brillouin zone is sampled using a 3 × 3 × 1 Γ-centered k-point, and the kinetic cut-off energy for the plane-wave basis set is 400 eV, with all calculations taking dispersion corrections into consideration using Grimme's DFT-D3 method [4]. For multi-layered Sv-ZIS, the bottom three layers atoms have been frozen to simulate the reaction surface, and when the maximum forces on the relaxed atoms are all less than 0.05 eV/Å, the structural optimization task is considered successful. Besides, a vacuum layer at least 15 Å is set up to avoid the mirror interaction of adjacent cells.

5. Characterization

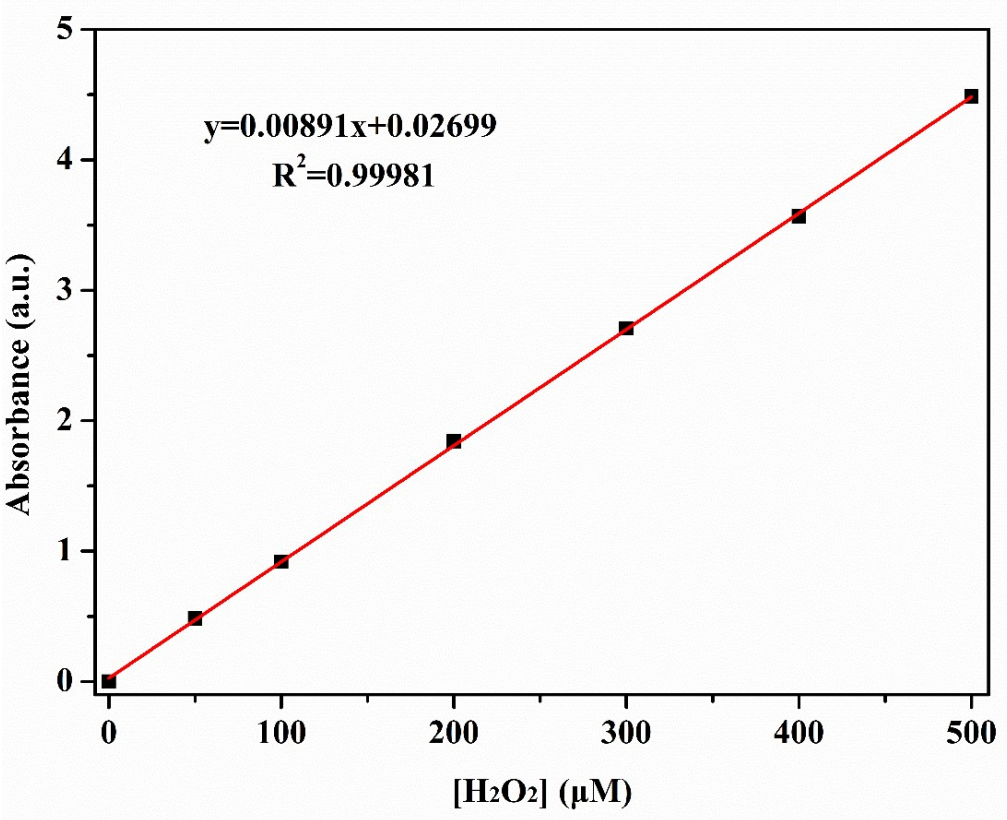

Fig. S1. The standard curve of H_2O_2 concentration.

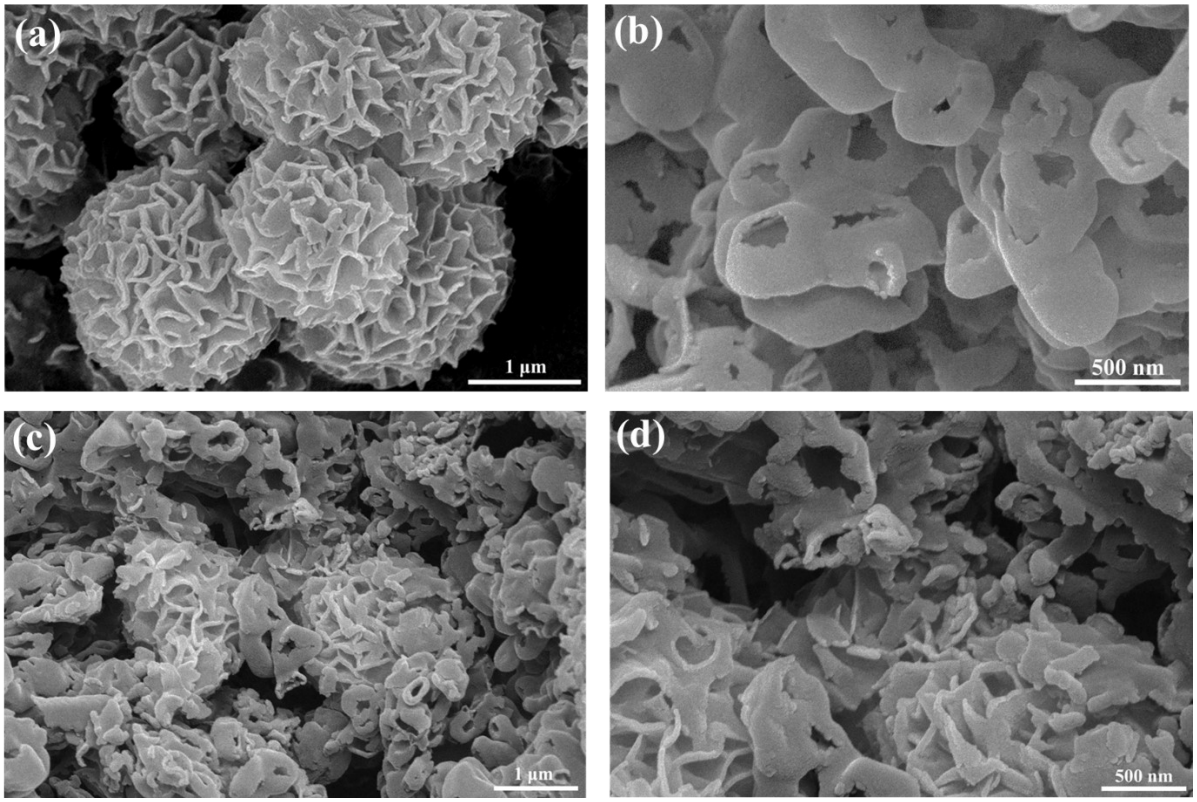

Fig. S2. SEM images of (a) Sv-ZIS; (b) 3DA-CN; (c, d) Sv-ZIS/CN.

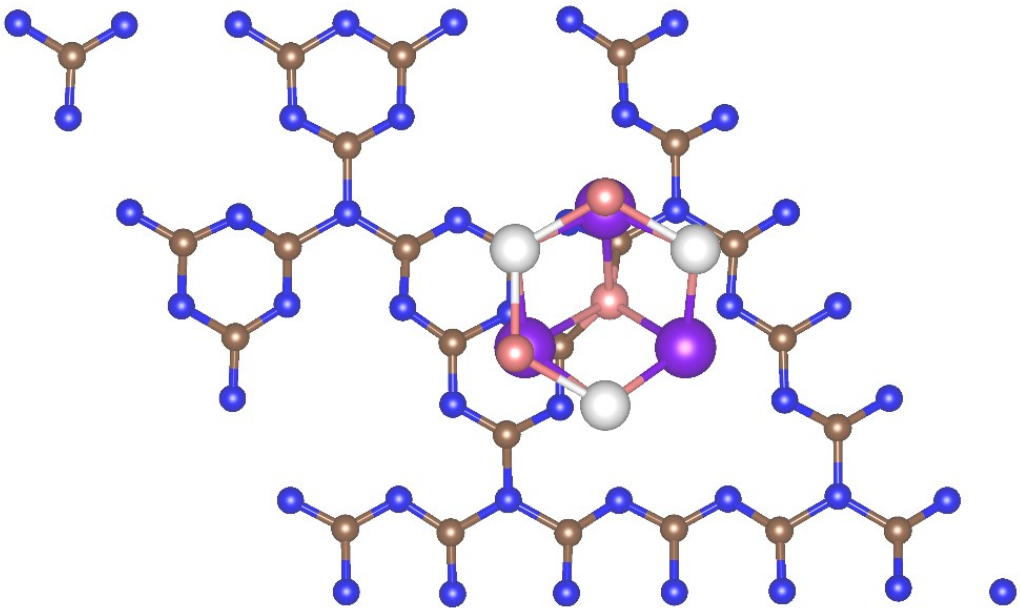

Fig. S3. The top view optimized structure model of Sv-ZIS/CN.

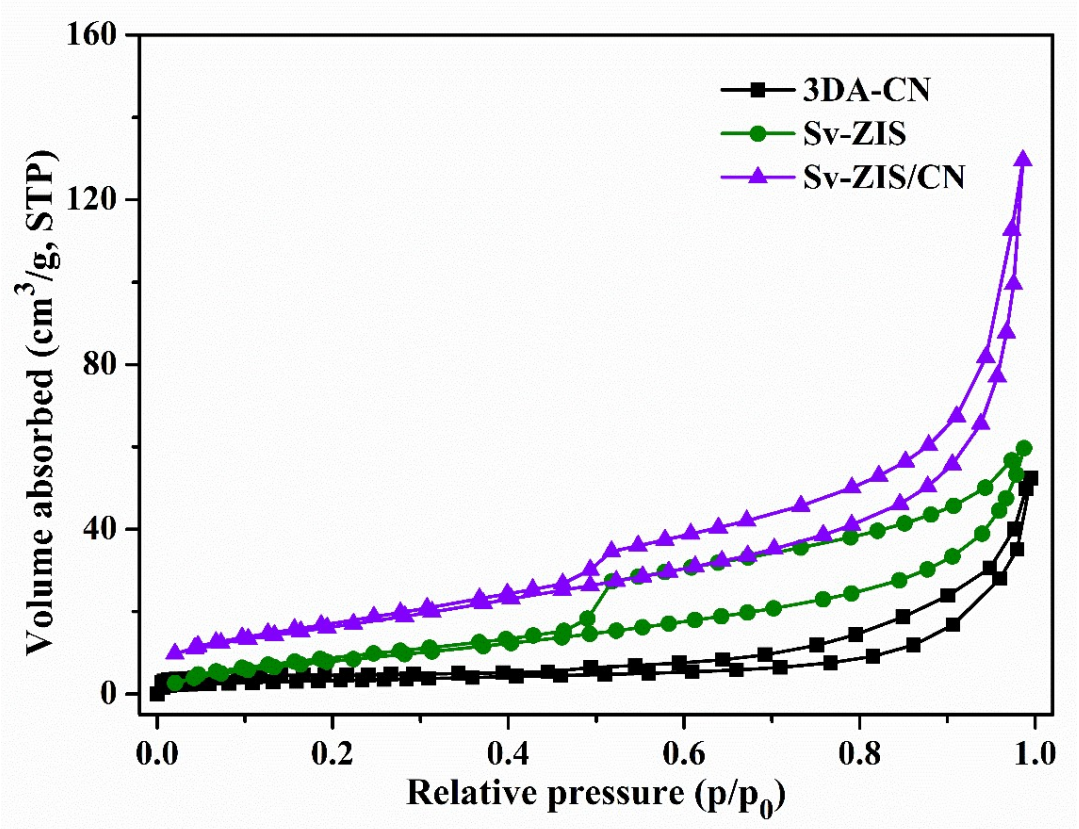

Fig. S4. N_2 adsorption-desorption isotherms of 3DA-CN, Sv-ZIS and Sv-ZIS/CN.

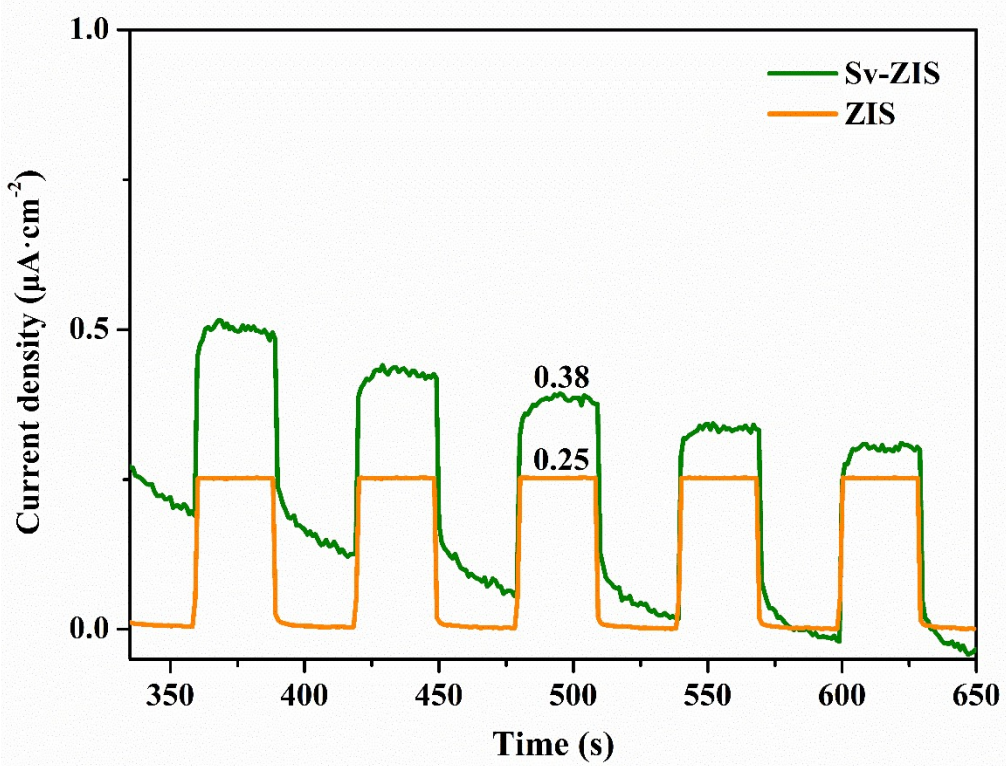

Fig. S5. The transient photocurrent response of Sv-ZIS and ZIS.

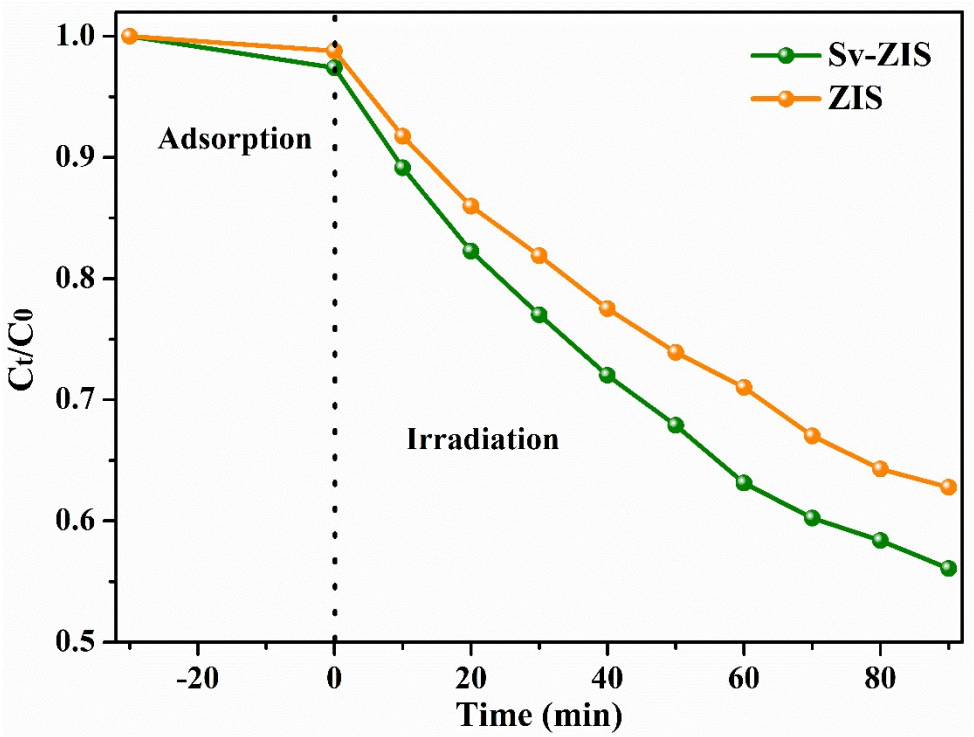

Fig. S6. Time-concentration plots of Sv-ZIS and ZIS for TC photocatalytic degradation.

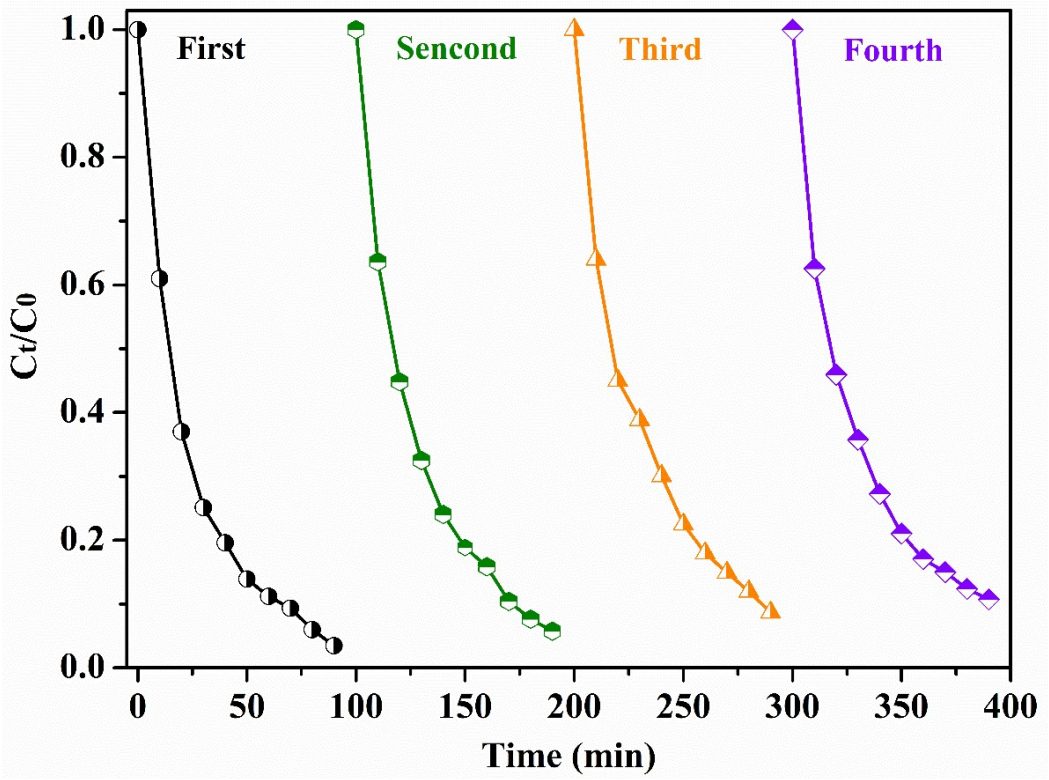

Fig. S7. The cycle degradation experiments of 4Sv-ZIS/CN.

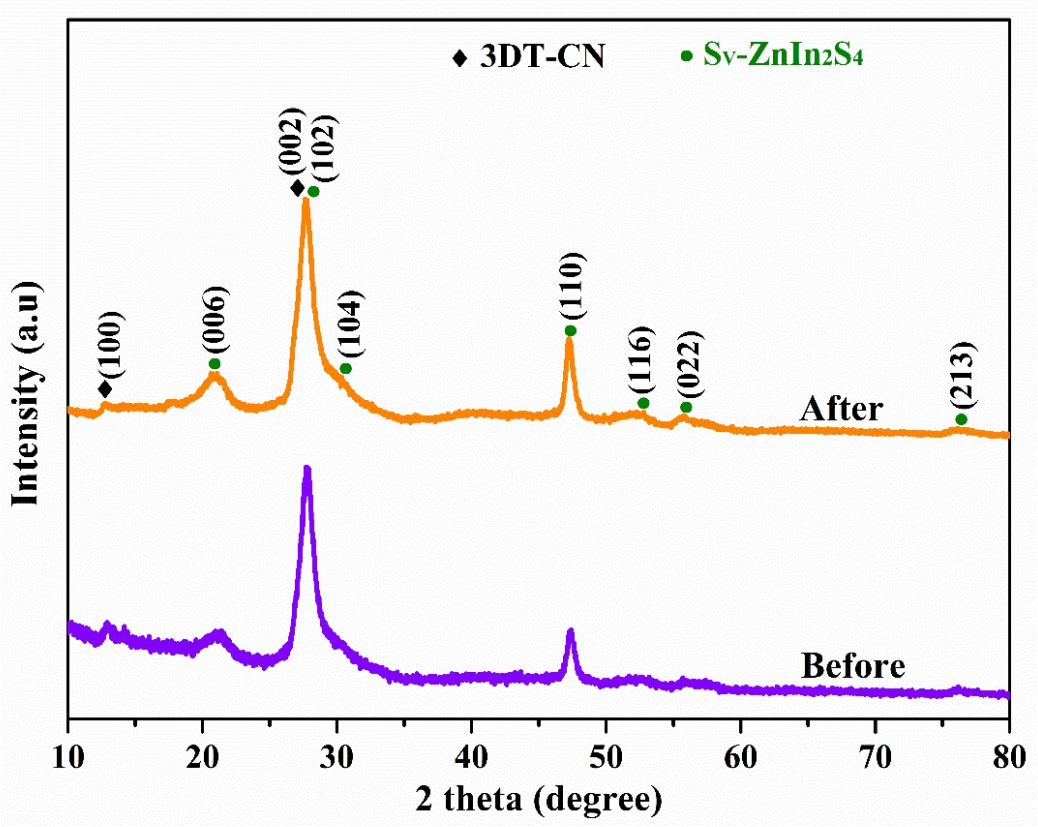

Fig. S8. The XRD patterns of 4Sv-ZIS/CN before and after photocatalytic degradation reaction.

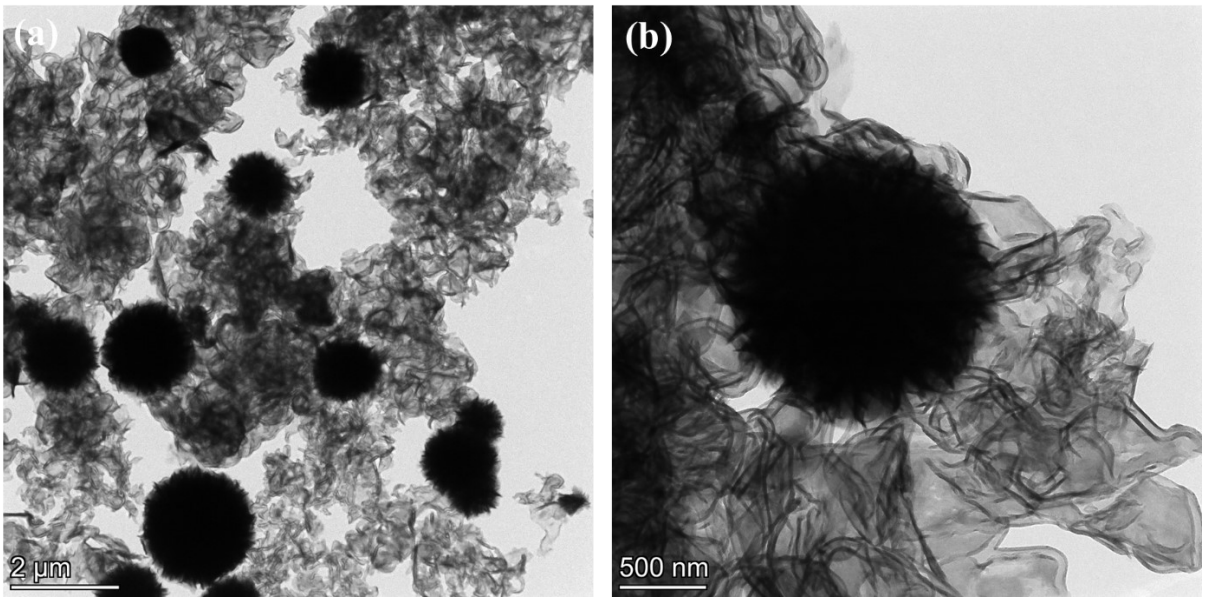

Fig. S9. (a, b) TEM images of 4Sv-ZIS/CN after four cycles of experiments.

6. Table of contents:

Table S1. Specific surface area of 3DA-CN, Sv-ZIS and Sv-ZIS/CN.

Products	S_{BET} ($m^2 \cdot g^{-1}$)
3DA-CN	**93.47**
Sv-ZIS	**191.40**
Sv-ZIS/CN	**137.52**

7. References

[1] G. Kresse, J. Furthmüller, *Comput. Mater. Sci.*, 1996, **6** 15–50.

[2] J.P. Perdew, K. Burke, M. Ernzerhof, *Phys. Rev. Lett.*, 1996, **77,** 3865–3868.

[3] G. Kresse, D. Joubert, *Phys. Rev. B*, 1999, **59,** 1758–1775.

[4] S. Grimme, J. Antony, S. Ehrlich, H. Krieg, *J. Chem. Phys.*, 2010, **132** 154104.